ASSESSMENT OF ARTIFICIAL NEURAL NETWORK FOR BATHYMETRY ESTIMATION USING HIGH RESOLUTION SATELLITE IMAGERY IN SHALLOW LAKES: CASE STUDY EL BURULLUS LAKE.

Hassan Mohamed[1], AbdelazimNegm[2], Mohamed Zahran[3], and Oliver C. Saavedra[4]

[1] PhD Student, Department of Environmental Engineering, Egypt-Japan University of Science and Technology E-JUST, New Borg El-Arab, Alexandria, Egypt, E-mail: hassan.mohamed@ejust.edu.eg

[2] Chairperson of Department of Environmental Engineering, Egypt-Japan University of Science and Technology E- JUST, New Borg El-Arab, Alexandria, Egypt, E-mail: negm@ejust.edu.eg (seconded (from Zagazig University, amnegm@zu.edu.eg

[3] Chairperson of Surveying Engineering Dept., Faculty of Engineering at Shoubra, Benha University, Egypt, Email: mohamed.zahran01@feng.bu.edu.eg

[4] Department of Civil Engineering, Graduate School of Science and Engineering, Tokyo Institute of Technology, Tokyo, Email: saavedra.o.aa@m.titech.ac.jp

ABSTRACT

In this research, an approach for estimating shallow water depths (bathymetric map) from multispectral images is proposed. This method is based on using Artificial Neural Network (ANN) fitting algorithms using reflectance of influencing bands of water depths and their logarithms for bathymetry detection. An automated method for calibrating the parameters for a Log- Nonlinear inversion model was developed using Levenberg-Marquardt training algorithm. The ANN fitting algorithms using reflectance of Green and Red bands and their logarithms was compared with ANN using reflectance of four SPOT-4 image bands, ANN using reflectance of Green band only and two other conventional models. These are third order polynomial correlation using the Reflectance of Green band and Generalized Linear Model (GLM) using reflectance of both Green and Red bands. The retrieved bathymetry from all methods using SPOT image was evaluated by Echo Sounder data. The results showed that the proposed approach using reflectance of Green and Red bands and their logarithms has acceptable performance and more accurate than other methods with RMSE of 0.15 m. The methods of ANNs with single layer model, using reflectance of four bands, 3rd order polynomial and GLM gives RMSE of 0.17 m, 0.165 m, 0.19 m and 0.18 m respectively over shallow water depths less than 2m.

KEYWORDS: Bathymetry; Neural Network, Satellite imagery; Spot.
Received 13 March 2015.Accepted 21, september 2015
Presented in IWTC 18th

1 INTRODUCTION

Bathymetric information is key element in many applications such as Hydrographic surveying, coastal engineering applications, sustainable marine planning and management and shipping traffic safety (Gao 2009; Leu and Chang 2005; Jupp 1989). Many near/off shore activities and Hydrological studies needs accurate water depths such as Hydrology, sedimentary processes and sediment transportation in coastal zones (Lyzenga 1978, 1985; Klemas 2009), mineral exploration (Basu and Malhotra 2002), hydrodynamic models development (Sutherland et al. 2004), mapping different types of submerged reefs on the seafloor (Brock et al. 2004) and benthic habitat maps (Mishra et al. 2006).

Ship-borne surveys with single or multi-beam echo sounders have been used conventionally to measure water depths up to 500 m. Some methodologies were developed using Vertical Beam Echo-Sounder (VBES) bathymetric data acquisition and post processing to obtain the full bottom bathymetry (Sánchez et al. 2012). In addition, Multi-beam echo-sounders provide full bottom coverage with about 8 cm depth accuracy in 200 m water depth (Kongsberg 2005). However, many

shallow water areas are not accessible by hydrographic vessels due to the shallowness of the water, bottom rocks and coral reefs (Mehdi et al. 2013). Moreover, ship-borne surveys are time consuming, costy and needs intensive labor particularly in relatively shallow coastal waters where survey swaths are narrow (Su et al. 2008).

Recently, Airborne Lidar technology has been developed for mapping shallow coastal areas. Although this technology provides very accurate bathymetry and excellent results (Chust et al. 2010) with about 20 cm vertical accuracy in depth measurements up to 30 m, their use is limited by their high costs and comparatively limited coverage.

Optical remote sensing relying on passive multispectral scanner data has provided a cost, wide coverage and time-effective solution for accurate bathymetry (Lyzenga 1985; Stumpf et al. 2003; Su et al. 2008). The first uses of the remote sensing technology in estimating water depths from combination of aerial multispectral data and radiometric techniques over clear shallow water was by Lyzenga (1978). After lunching Landsat satellites this technique was applied on Landsat images (Van and Daniel 1991). In the following years, many satellites were lunched with higher spatial and radiometric resolution and also used in bathymetric applications. For instance, Ikonos (Su et al. 2008), Quickbird (Lyons et al. 2011), and Worldview-2 (Georgia et al. 2012).

During the last decades, various depth estimation methods based on establishing a relationship between image pixel values and known water depth values were developed. Lyzenga (1978; 1981; 1985) developed bathymetry algorithms for a single wavelength band and a pair of wavelength bands based on linear relationships derived from the Lambert-Beer equation of attenuation. His theory is based on the correction of sun glint effect using the near infrared NIR band and the removal of the water column. Stumpf et al. (2003) proposed a novel algorithm based on the ratio of bands reflectance and proved its benefits to retrieve depths especially in deep water comparing with standard linear transform algorithm. In the following years both models were developed by other researches. Lyzenga's algorithms were developed later by Conger et al. (2006) using single colour band integrated with LIDAR bathymetry data and (Stumpf et al. 2003) algorithm was developed later by Su et al. (2008) using an automated method for calibrating the ratio model parameters.

The limitation of these algorithms is that they rely on the assumption that water optical properties like attenuation and quality are the same for the image scene and that the ratio of bottom reflectance in spectral bands is the same for different types of bottoms within a given scene. Thus, if this assumption is not achieved in some areas the estimated depths will have intrinsic errors. The ideal conditions for these models are high clarity and uniform water quality and bottom type for the whole scene (Su et al. 2008).

In the last few years, ANNs algorithms were used for bathymetry detection by many researchers. Özçelik and Arısoy (2010) used ANNs for detecting the nonlinear relationship between reflectance from different spectral bands and water depths. These algorithms isolate water attenuation and hence depth from other environmental factors as bottom material and vegetation by using different combinations of spectral bands. The same algorithm was applied by other researchers using different satellite images and different areas such as (Mehdi et al. 2013) using MLP-ANNs method for Landsat images, (Sheela et al. 2013) for (IRS P6-LISS III) satellite images. (Linda et al. 2011) used neuro-fuzzy approach for Quickbird images.

Although these methods gives more reliable results and have several advantages than conventional models (Özçelik and Arısoy 2010) they have some limitations. They needs a large number of spectral bands which leads to over needs data as instance NIR bands which does not contain bottom-reflected signal so its insignificant for bathymetry applications (Georgia et al. 2012) or other bands which have no influence in different depths estimation. Also some areas needs atmospheric and sun glint pre-corrections which influence the derived bathymetry.

The objective of this research is to propose a methodology for bathymetry detection using only the influencing bands for bathymetry after removing atmosphere and sun glint corrections and their logarithms as input data in ANNs. The proposed methodology exploits the advantages of other approaches and overcome their limitations. Applying atmosphere and sun glint corrections reduces their influence on detected depths and using ANNs reduces the required depth measurements, yielding fast and reliable water depths. The methodology was applied using SPOT imagery of EL-Burullus Lake in Egypt and compared with other methods. Achieved results were evaluated using Echo-Sounder bathymetric data for the same area.

2 MATERIALS AND METHODS

2.1. Study area and Materials

The study area is Lake Burullus which extends along the northern part of the Nile Delta, Egypt with 65 km length in the E–W direction and 11 km average width in the N–S direction (Figure 1). It's a shallow lake with depths from 0.4 m to 2 m and the shallowest part of the lake is the eastern sector with depths from 0.75m to 1 m (Ali 2011).

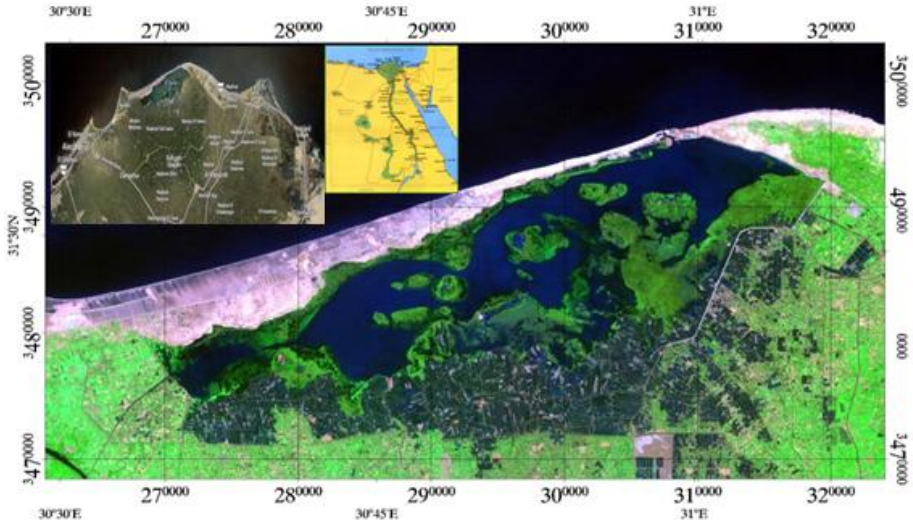

Figure 1: The study area El-Burullus Lake, Nile-Delta, Egypt (Ahmed et al. 2013).

A SPOT-4 HRG 2 pan-sharped satellite image with four multispectral bands is used for detecting bathymetry for the study area. The four bands are green (0.5–0.59 µm), red (0.61–0.68 µm), near-infrared (0.78–0.89 µm) and short-wave infrared (1.58–1.75 µm). The image has 10 m spatial resolution and was acquired on July 1st, 2012 (see Figure 2).

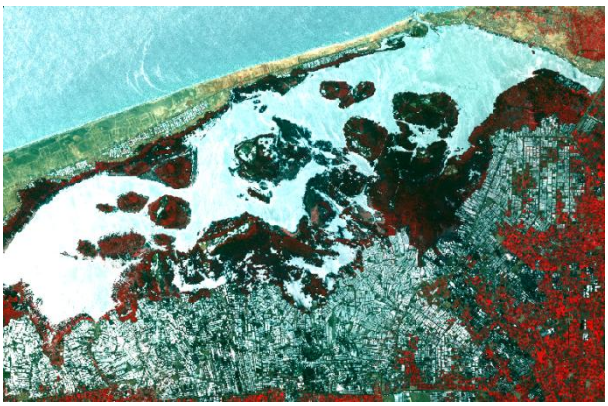

Figure 2; The SPOT-4 satellite image of the study area (July 1st, 2012).

The reference data for bathymetry was acquired by Echo-Sounder instrument (see Figure 3).

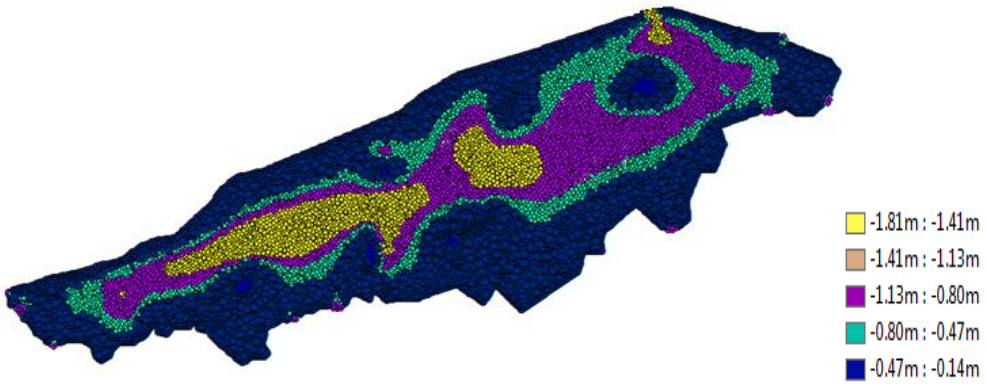

Figure 3: Reference bathymetry points from Echo-Sounder.

2.2. Methods

The following subsections describe the methodology used in this research.

2.2.1. Imagery data pre-processing

The phases of imagery data processing can be written as follow.

2.2.1.1. Converting the image pixel digital numbers to radiance values using the gain and bias information of sensor bands using Eq.1:

$L\lambda = DN\ (Gain) + Bias$ (1)

Where: $L\lambda$ = Radiance values for each band
DN = digital numbers recorded by the sensor
Gain = the gradient of the calibration
Bias = the spectral radiance of the sensor for a DN of zero (Amr et al. 2013).
Both gain and bias values were available in the image metadata file.

2.2.1.2. Computing the reflectance of each pixel value using the radiances computed in Eq.2:

$$\boldsymbol{\rho}\lambda = \frac{\pi\ d2\ L\lambda}{Eo\lambda\ \cos\ \theta s} \quad (2)$$

Where: $\boldsymbol{\rho}\lambda$ = the reflectance as a function of band width λ
d^2 = the square value of Earth-sun distance correction (in atmospheric units)
$Eo\lambda$ = exoatmospheric spectral irradiance for each band and
θs = solar zenith angle

The earth-sun distance correction for the acquired imagery date is d=1.01667 (Landsat-7 2011), $Eo\lambda$ for each band of SPOT-4 image and θs can be found in the image metadata file (Amr et al. 2013).

2.2.1.3. Applying atmospheric correction for the image using dark pixel subtraction which is the preferred method for bathymetry detection (Mishra et al. 2004). The corrected pixel value can be calculated using Eq.3 as follow (Georgia et al. 2012):

$R_{ac} = R_i - R_{dp}$ (3)

Where: R_{ac}= corrected pixel reflectance value

R_i = initial pixel reflectance value

R_{dp} = the dark pixel value.

Any error in determination of R_{dp} may influence the depth estimation values (Stumpf et al. 2003).

2.2.1.4. Applying Sun Glint correction using the relation between Near-infrared band and other bands (Hedley et al. 2005; Noela et al. 2014). The de-glinted pixel value can be easily determined using Eq.4 as follow:

$$R_i' = R_i * b_i (R_{NIR} - Min_{NIR}) \quad (4)$$

Where: R_i' = de-glinted pixel reflectance value
R_i = initial pixel reflectance value
b_i = regression line slope
R_{NIR} = corresponding pixel value in NIR band
Min_{NIR} = min NIR value existing in the sample.

The accuracy of results relies on choosing varying dark, deep and has glint areas pixel samples from the imagery water region (Edwards 2010).

2.3. ANN methodology for bathymetry estimation

ANN is a processing model for information emulating the same way which densely interconnected parallel structure of the brain processes information. ANN information processing system consists of large number of highly connected processing elements like neurons tied together with weighted connections like synapses (Mas 2004). The ability to handle non-linear functions, flexible approximation for many types of data, learn from unseen data relationships and observed data are some of ANN main advantages. It's a powerful tool that can be used for many applications as image processing, environmental science, medicine, ecological and molecular biology… etc. (Özçelik and Arısoy 2010; Mas 2004).

Multilayer Feed-Forward or (Multilayer Perceptron) Neural Network Algorithm was used in this study. Its poplar supervised approach, widely used in displaying the non-linear relationship between input and output data (Rumelhart et al. 1986). Multilayer Perceptron Network (MLP) consists of three parts: the input layers as neurons which represent the available data in this case the multispectral image band values, the hidden layer which demonstrate the network training process and finally the output layer which will be the bathymetric information. A hypothetical example of (MLP) ANNs with 4 input layers, 5 hidden layers and one output layer (4-5-1) is demonstrated in Figure 4.

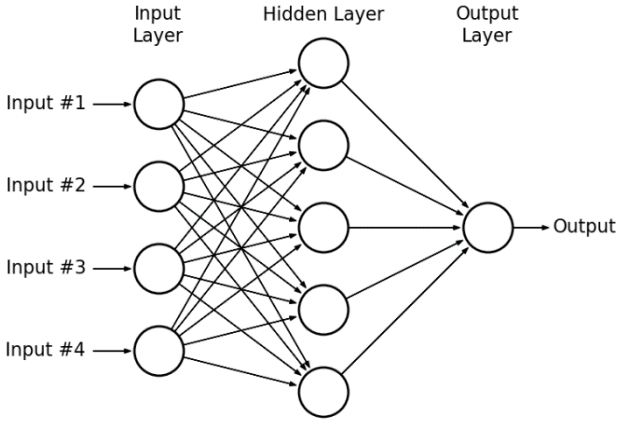

Figure 4: A hypothetical example of Multilayer Perceptron Network.

Error back-propagation learning algorithm is used for training data in Multilayer Perceptron Network. It starts with initial network weights which are adjusted as gradient then the training algorithm attempts to find the least error values through comparing desired and actual outputs in a repeatable process until the network reaches acceptable values (Behzad 2014; Gardner et al. 1998).

The log sigmoid function was used for transferring the net input net_j into the node outputs o_j as it's easily computed derivative and commonly used as follow:

$$f(net_j) = \frac{1}{(1+exp\,(-net\,j))} \quad (5)$$

The training algorithm of Levenberg-Marquard was used in this study for weight and bias values updating. It's the fastest back propagation algorithm and is highly recommended as a first-choice supervised algorithm used for training moderate-sized feed forward neural networks which can be extended up to several hundred of weights (Ananth 2004). The algorithms is given in Eq.6 (Özçelik and Arısoy 2010; Hagan and Menhaj 1994).

$$X_{k+1} = X_k + [J^T J + \mu I]^{-1} J^T \varepsilon_k \quad (6)$$

Where: X_k = vector of current weights and biases
ε = the vector matrix of the network errors
J = Jacobean matrix of the network errors
μ = scalar indicates calculation speed of the Jacobean matrix
k = iteration number
I = the unit matrix
T= the transpose matrix

3 RESULTS AND DISCUSSION

The SPOT-4 image was prepared for water depths estimation by firstly converting image pixel values to radiances then to reflectance using image metadata file values using Gain-Offset tool and band math tool using equation (2) respectively. Second, the atmospheric correction and sun-glint removal were applied to image reflectance values using Dark pixel subtraction tool and de-glint tool respectively. These two steps were performed in Envi software environment.

The proposed method was compared with four methods used previously 3rd order polynomial, Generalized Linear Model, ANNs with single band using green band which considered the most influenced band wavelength with water depths and ANNs with all visible bands to prove its validation as follow:

3.1. The nonlinear 3rd order polynomial correlation between the green band logarithm (L_G) and water depths in the form:

$$Z = 61.67 + 108.6\, L_G + 63.56\, L_G^2 + 12.51\, L_G^3 \quad (7)$$

With $R^2 = 0.512$ the 3rd order polynomial continuous fitted model showed in Figure 5.

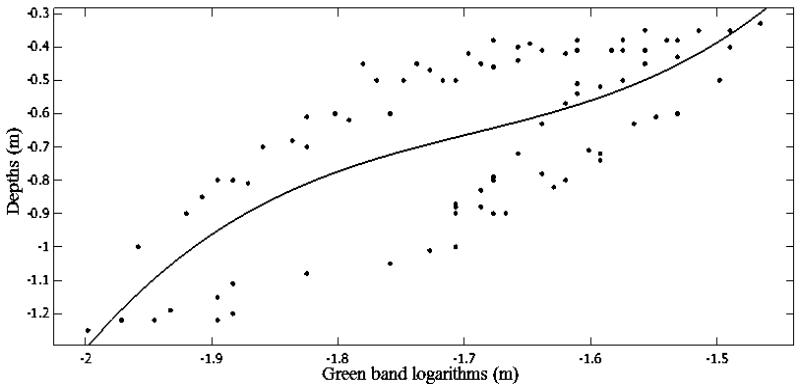

Figure 5: 3rd order polynomial continuous fitted model. Depths are represented as points and continuous line represents the fitted continuous model.

3.2. The Generalized Linear Model representing least-squares fit of the link of the response to the data. GLM links a linear combination of green and red corrected bands (GB, RB)and their logarithms (L_G, L_R) to the water depths values in the form:

$$Z = 1050.8 + 17562\ GB - 12903\ RB + 5.7432\ L_G - 14.6\ L_r - 7211.8\ GB\ RB - 5863.1\ GB\ L_G + 9543.7\ RB\ L_r + 8188.8\ GB\ L_r - 7139.7\ RB\ L_G - 72.058\ L_G\ L_r. \quad (8)$$

With $R^2 = 0.527$ GLM fitted continuous model showed in Figure 6.

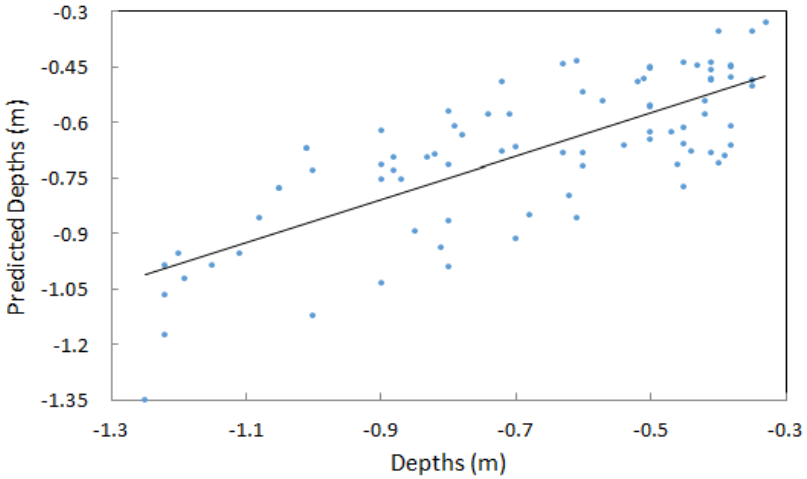

Figure 6; GLM continuous fitted model. Depths are represented as points and continuous line represents the fitted continuous model.

3.3. Supervised Multi-Layer Perceptron back propagation model with Levenberg-Marquard training algorithm learning ANNs using single green band logarithms as input layer and Water depths as output layer with 80% of data set for learning, 10% for validation and 10% for testing. The Log-sigmoid function was used for hidden layer and linear function for output layer. After many experiments with trial and error, the number of hidden layer neurons was determined based on the least RMSE and found to be 10 neurons. This number was fixed for all ANNs models. So the Network structure was (1-10-1).

With $R^2 = 0.572$ ANNs with single green band logarithms showed in Figure 7.

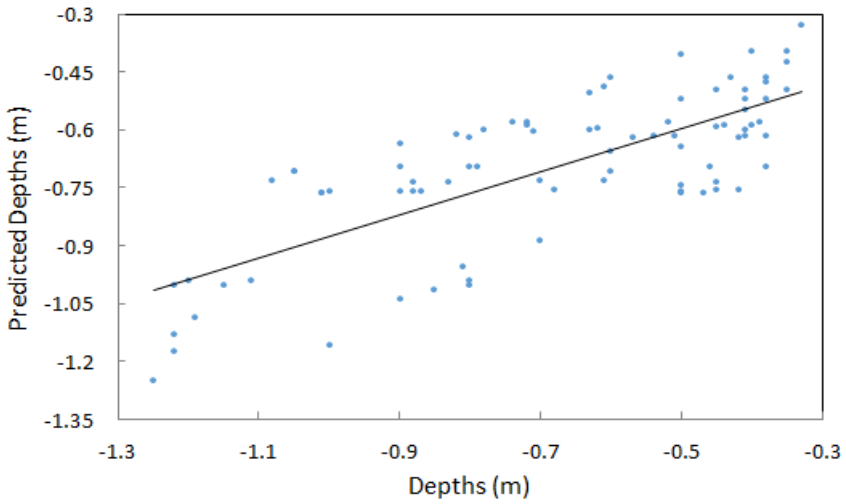

Figure 7: ANNs with single green band logarithms continuous fitted model. Depths are represented as points and continuous line represents the fitted continuous model.

3.4. Supervised ANNs Multi-Layer Perceptron back propagation model with Levenberg-Marquard training algorithm learning using four bands as input layer and Water depths as output layer with 80% of data set for learning, 10% for validation and 10% for testing. The Log-sigmoid function was used

for hidden layer with 10 neurons and linear function for output layer. The Network structure was (4-10-1).

With R^2 = 0.601 ANNs with four band showed in Figure 8.

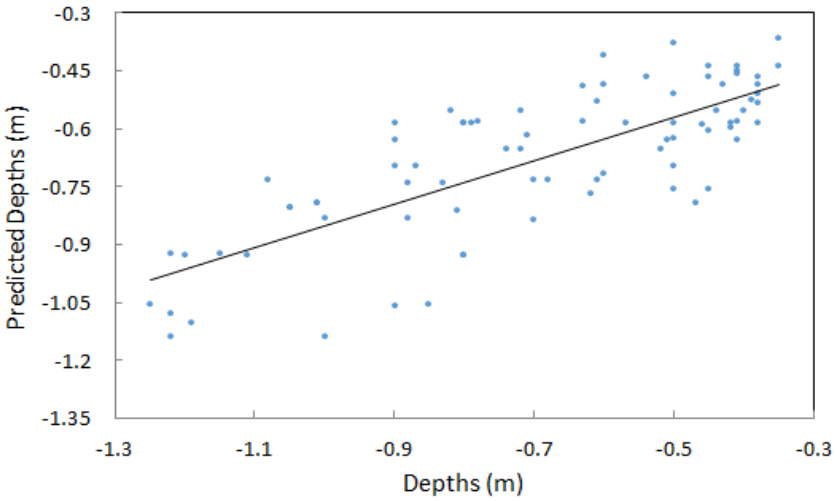

Figure 8: ANNs with four bands continuous fitted model. Depths are represented as points and continuous line represents the fitted continuous model.

3.5. The new proposed method for bathymetry detection is using only the influencing bands for bathymetry (green and red) and their logarithms as input layers in ANNs and water depths as output layer with 80% of data set for learning, 10% for validation and 10% for testing. The Log-sigmoid function was used for hidden layer with 10 neurons and linear function for output layer. The Network structure was (4-10-1).

With R^2 = 0.662 ANNs with four band showed in Figure 9.

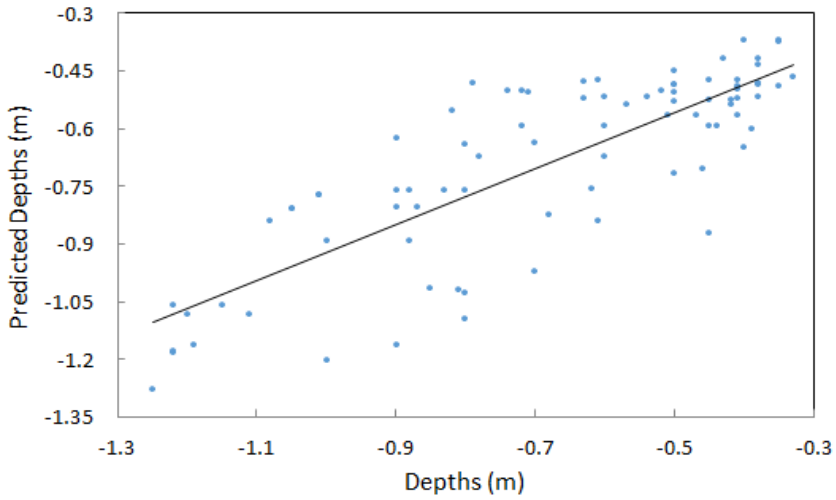

Figure 9. ANNs with four layers green, red bands with their logarithms continuous fitted model. Depths are represented as points and continuous line represents the fitted continuous model.

The Root Mean Square Error values of all methods were computed using the difference between each model values and actual depths. They are tabulated in Table 1.

Table 1. The Root Mean Square Error of estimated depths for all methods.

Methodology	3rd order Polynomial with Green band	GLM with Green and Red bands	ANNs with Green band Logarithm	ANNs with all bands	ANNs with both Green band, Red band and their Logarithms
RMSE	0.19 m	0.18 m	0.17 m	0.165 m	0.15 m

For comparing these results with previous studies many factors should be included as spatial resolution of satellite image, depths of the study area, water quality and availability of field water depths. Recently, Noela [27] prove the outperforming of GLM to 3rd order polynomial approach using Spot images. In addition many other studies prove the overall precedency of ANNs to Conventional approaches as Mehdi [25], Ozçelik [29]. These results demonstrate the outperforming of the proposed approach using influencing bands of bathymetry corrected from sun glint and atmospheric errors as an input for ANN to ANNs using all visible bands.

4 CONCLUSION

The main contribution of this research is proposing a methodology for bathymetry which was validate in Lake EL-Burullus, Egypt. The proposed methodology uses bands corrected from atmospheric and sun-glint systematic errors which influencing bathymetry and their logarithms as an input layer in Multi-Layer Perceptron Neural Network. To validate proposed methodology four different approaches using SPOT-4 satellite image for shallow Lake EL-Burullus with depths less than 2 m was carried out. All approaches were tested by Echo-Sounder data of water depths. The first approach; 3rd order polynomial correlation algorithm using the reflectance of green band gave RMSE of 0.19 m. GLM with reflectance of Green, Red band and their logarithms yielded RMSE of 0.18 m. ANNs using reflectance of green band only as input layer in MLP resulted in RMSE of 0.17 m. The fourth approach; ANNs using reflectance of all four SPOT image bands as input layer for MLP yielded RMSE of 0.165 m. The proposed methodology gave RMSE of 0.15 m which outperformed aforementioned methods. It can be concluded that ANNs gives more accurate results than conventional methods for bathymetric applications and the proposed approach has precedency to other ANNs.

5 ACKNOWLEDGMENTS

The first author would like to thank Egyptian Ministry of Higher Education (MoHE) for providing him the financial support (PhD scholarship) for this research as well as the Egypt Japan University of Science and Technology (E- JUST) and JICA for offering the facility and tools needed to conduct this work.This study was partially supported by JSPS Core-to-Core Program, B.Asia-Africa Science Platforms.

REFERENCES

Ahmed, E.; Negm, A.; M., Elzeir; Oliver. C.; I., El-Shinnawy; Kazuo, N. (2013) "Modeling the Hydrodynamics and Salinity of El-Burullus Lake (Nile Delta, Northern Egypt)",*Journal of Clean Energy Technologies*, Vol. 1, pp.157-163.

Ali E. (2011) "Impact of drain water on water quality and eutrophication status of Lake Burullus, Egypt, a southern Mediterranean lagoon",*African Journal of Aquatic Science*, Vol. 36, pp. 267–277.

Amr F.; Chihiro Y.; Oliver S.; Ahmed T.; Zuliziana S. (2013)"Suspended Sediment Load Monitoring Along the Mekong River from Satellite Images",*Journal of Earth Science & Climatic Change*, Vol. 4, pp. 1-6.

Ananth R. (2004) "The Levenberg-Marquardt Algorithm.8",Available: http://www.ananth.in/Notes_files/lmtut.pdf.

Atanu B.; Shivani M. (2002) "Error Detection of Bathymetry Data by Visualization Using GIS", ICES *Journal of Marine Science*, Vol. 59, pp. 226–234.

Behzad S. (2014) "Predicting the Trend of Land Use Changes Using Artificial Neural Network and Markov Chain Model (Case Study: Kermanshah City)",*Research Journal of Environmental and Earth Sciences*, Vol. 6, pp. 215-226.

Brock, J.; C. Wright; T. Clayton; A. Nayegandhi. (2004) "LIDAR optical rugosity of coral reefs in Biscayne National Park",*Florida. Coral Reefs*, 23, 48–59.

Chust, G.; M. Grande; I. Galparsoro; A. Uriarte; A. Borja. (2010) "Capabilities of the Bathymetric Hawk Eye LIDAR for Coastal Habitat Mapping: A Case Study within a Basque Estuary",*Estuarine, Coastal and Shelf Science*, Vol. 89, pp. 200–213.

Edwards A., Les. 5: (2010) "Removing sun glint from compact airborne spectrographic imager (CASI) imagery",Bilko 3, module 7, Available: http://www.noc.soton.ac.uk/bilko/module7/m7_15.php.

Gao J. (2009) "Bathymetric Mapping By Means Of Remote Sensing: Methods, Accuracy and Limitations",*Progress in Physical Geography*. Vol. 33, pp. 103–116.

Gardner M.; Dorling S. (1998) "Artificial Neural Networks the Multilayer Perceptron - Review of Application in Atmospheric Science",*Atmospheric Environmental*. Vol. 32, pp. 2627-2636.

Georgia. D.; M. Papadopouloua; P. Lafazania; C. Pikridasb; M. Tsakiri-Stratia. (2012) "Shallow-water bathymetry over variable bottom types using multispectral Worldview-2 image",*International Archives of the Photogrammetry, Remote Sensing and Spatial Information Sciences*, Vol. XXXIX-B8, XXII ISPRS Congress, 25 August – 01 September 2012, Melbourne, Australia.

Hagan, M.; Menhaj M. (1994) "Training feed forward networks with the Marquardt algorithm",*IEEE Transactions on Neural Networks*,Vol. 5, pp. 989-993.

Jupp, D. (1988) "Background and extension to depth of penetration (DOP) mapping in shallow coastal waters",*Presented at the Symposium of Remote Sensing of the Coastal Zone*, pp. IV.2.1-IV.2.19, Gold Coast, Queensland.

Klemas, V. (2009) "Remote Sensing of Coastal Resources and Environment",*Environmental Research, Engineering and Management*, Vol. 2, pp. 11–18.

Kongsberg. (2007) "EM120 multi-beam echo sounder",Available: http://www.knogsberg.com.

Landsat-7. (2011) "Landsat Science Data Users Handbook", http://landsathandbook.gsfc.nasa.gov/data_prod/prog_sect11_3.html, (Accessed 20 July 2014).

Leu, L.; Chang, H. (2005) "Remotely sensing in detecting the water depths and bed load of shallow waters and their changes",*Ocean Engineering*, Vol. 32, pp. 1174-1198.

Linda C.; Andrea M.; Marco C. (2011) "Approaching bathymetry estimation from high resolution multispectral satellite images using a neuro-fuzzy technique",*Journal of Applied Remote Sensing*, Vol. 5, pp. 0535151-05351515.

Lyons M.; Phinn S.; C. Roelfsema. (2011) "Integrating Quickbird multi-spectral satellite and field data: Mapping bathymetry, Seagrass Cover, Seagrass species and change in Moreton bay",*Remote Sens.*, Vol. 3, pp. 42-64.

Lyzenga, D. (1978) "Passive remote sensing techniques for mapping water depth and bottom features",*Applied Optics*, Vol. 17, pp. 379-383.

Lyzenga D. (1981) "Remote sensing of bottom reflectance and other attenuation parameters in shallow water using aircraft and Landsat data",*Int. J. of Remote Sensing*, Vol. 2, pp. 71-82.

Lyzenga, D. (1985) "Shallow-water bathymetry using combined Lidar and passive multispectral scanner data",*International Journal of Remote Sensing*, Vol. 6, pp. 15-125.

Mas J. (2004) "Mapping land use/cover in a tropical coastal area using satellite sensor data, GIS and Artificial Neural Networks",*Estuarine, Coastal and Shelf Science*, Vol. 59, pp. 219-230.

Mehdi G.; 1, Tiit K.; Abbas E.; Ali A.; Babak N. (2013) "Remotely Sensed Empirical Modeling of Bathymetry in the Southeastern Caspian Sea",*Remote Sens.*, Vol. 5, pp. 2746-2762.

Mishra, D.; S. Narumalani; D. Rundqulst; M. Lawson. (2006) "Benthic habitat mapping in tropical marine environments using QuickBird multispectral data",*Photogrammetric Engineering & Remote Sensing*, Vol. 72, pp. 1037–1048.

Noela S.; José O.; Daniel R.; José M. (2014) "Assessment of different models for bathymetry calculation using SPOT multispectral images in a high-turbidity area: the mouth of the Guadiana Estuary",*International Journal of Remote Sensing*, Vol. 35, pp. 493–514.

Noela S.; S. Aceña; Daniel R.; E. Couñago; P. Fraile; J. Freire. (2012) "Fast and low-cost method for VBES bathymetry generation in coastal areas",*Estuarine, Coastal and Shelf Science*, Vol. 114, pp. 175–182.

Ozçelik C.; Arısoy Y. (2010) "Remote sensing of water depths in shallow waters via artificial neural networks",*Estuar. Coast. Shelf Sci.*, 89, 89–96.

Rumelhart D.; Geoffrey E.; Robert J. (1986) "Learning Internal Representations by Error Propagation",*Rumelhart, D.E. and J.L. McClelland (Eds.), Parallel Distributed Processing*, Vol. 1, pp. 318-362 MIT Press, Cambridge.

Sheela A.; Letha J.; Sabu J.; Jairaj P; Justus J. (2013) "Lake bathymetry from Indian Remote Sensing (P6-LISS III) satellite imagery using artificial neural network model",*Lakes & Reservoirs: Research and Management*, Vol. 18, pp. 145–153.

Stumpf R.; Holderied K.; M. Sinclair. (2003) "Determination of water depth with high-resolution satellite imagery over variable bottom types",*Limnol. Oceanogr*.Vol. 48, pp. 547-556.

Su H.; Liu H.; W. Heyman. (2008) "Automated derivation for bathymetric information for multispectral satellite imagery using a non-linear inversion model",*Marine Geodesy*, Vol. 31, pp. 281-298.

Sutherland J.; D. Walstra; T. J. Chesher; L. van Rijn; H. Southgate. (2004) "Evaluation of Coastal Area Modeling Systems at an Estuary Mouth",*Coastal Engineering*, Vol. 51, pp. 119–142.

Van H.; Daniel. S. (1991) "Multi-temporal water depth mapping by means of Landsat TM",*Int. J. of Remote Sensing*, Vol. 12, pp. 703-712.